ON THE DESIGN AND IMPLMENTATION OF A CLASS OF MULTIPLIER-LESS TWO-CHANNEL 1-D AND 2-D NONSEPARABLE PR FIR FILTERBANKS

S. C. Chan, K. S. Pun and K. L. Ho
Department of Electrical and Electronic Engineering,
The University of Hong Kong, Pokfulam Road, Hong Kong.
Email: scchan@eee.hku.hk, kspun@eee.hku.hk, klho@eee.hku.hk

ABSTRACT

This paper proposes a new design and implementation method for a class of multiplier-less 2-channel 1D and 2D non-separable perfect reconstruction (PR) filter banks (FB). It is based on the structure proposed by Phoong *et al.* and the use of multiplier block (MB). The latter technique allows one to further reduce the number of adders in implementing these multiplier-less FB by almost 50%, compared to the conventional method using sum of powers of two coefficients (SOPOT) alone. Furthermore, by generalizing the 1D to 2D transformation of Phoong *et al.*, new 2D PR FBs with quincunx, hourglass, and parallelogram spectral support are obtained. These nonseparable FBs can be cascaded to realize new multiplier-less PR directional FB for image processing and motion analysis. Design examples are given to demonstrate the usefulness of the proposed method.

I. INTRODUCTION

Perfect reconstruction (PR) filter banks (FBs) have important applications in signal processing, signal coding and the construction of wavelet basis. Their design and efficient implementation are therefore of great interest [2][5][8][9]. In [2], a class of two-channel biorthogonal FB with the PR condition being structurally imposed was proposed [2]. More precisely, the filter bank is parameterized by two functions $\alpha(z)$ and $\beta(z)$, which can be chosen as FIR or IIR functions, without affecting the PR condition. Therefore, its design and implementation complexities are very low. Moreover, it was shown recently that nonlinear-phase PR FIR filter banks with low system delay can also be derived from this structure. The design of such low-delay and linear-phase PR FIR filter banks can be performed by the commonly used Remez exchange algorithm [5][6]. Another advantage of this class of filter banks is that they can be transformed, via a simple transformation, to obtain 2D PR FIR nonseparable filter banks with quincunx spectral support [2].

In this paper, we shall consider the multiplier-less implementation of such 2-channel PR FBs and their 2D nonseparable generalization. In particular, the coefficients in the FIR functions $\alpha(z)$ and $\beta(z)$ mentioned earlier are represented as sum of powers of two (SOPOT) representations [3], which can be implemented efficiently using only hard-wired shifters and adders. The construction of multiplier-less FIR/IIR FBs and wavelet basis, using this concept, were recently reported by the authors in [6]. It will be shown in this paper that the number of adders required can be further reduced by implementing the SOPOT coefficients of $\alpha(z)$ and $\beta(z)$ using a technique called Multiplier Block (MB) [4]. Multiplier block is a technique for reducing the number of adders required when the multiplicand is multiplied with a set of constant multipliers. In principle, it is possible to remove the redundancies in the constant multiplications leading to realization with minimum adders. To search for the SOPOT filter coefficients, a simple but effective algorithm based on random search is also proposed. It was found that the searching time of this simple algorithm is much lower than that of genetic algorithm (GA) [6][7], because of the availability of good real-valued solution. Design results show that low complexity SOPOT FBs with good frequency characteristic can be obtained by this approach. Using these 1D multiplier-less FBs, it is possible to construct 2D multiplier-less PR FB with quincunx, hourglass and parallelogram spectral support. Furthermore, these multiplier-less 2D nonseparable PR FBs can be cascaded appropriately in a tree-structure to obtain new PR multiplier-less directional filter banks, using the approach previously proposed in [1]. Such directional filters found important applications in segmentation, directional decomposition of images, motion analysis of videos, etc [1].

The paper is organized as follows: the proposed 1D multiplier-less SOPOT FB and its design procedure are introduced in sections II and III. Their generalizations to 2D linear-phase and nonlinear-phase nonseparable PR filter banks with quincunx, hourglass and parallelogram spectral support are discussed in Section IV. Conclusions are drawn in section V.

II. SOPOT FB USING MULTIPLIER BLOCK

The 2-channel structurally PR FB proposed in [2] is shown in fig. 5. ($\boldsymbol{E(z)}$ and $\boldsymbol{R(z)}$ are the polyphase matrices of the analysis and synthesis banks, respectively). It can be shown from fig. 5 that the z-transform of the analysis filters are

$$H_0(z) = \tfrac{1}{2}\left(z^{-2N} + z^{-1}\beta(z^2)\right),$$
$$\text{and} \qquad H_1(z) = -\alpha(z^2)H_0(z) + z^{-2M-1}. \qquad (1)$$

An interesting property of this FB is that it is PR for whatever choices of $\alpha(z)$ and $\beta(z)$. Therefore, they can be chosen as linear-phase or nonlinear-phase FIR functions. Interested readers are referred to [5] for the design of such FBs. In the proposed multiplier-less FB, each coefficient in $\alpha(z)$ and $\beta(z)$ is represented as the following SOPOT or canonical signed digits (CSD) representation [5],[6], $b = \sum_{k=0}^{L-1} a_k \cdot 2^{-b_k}$, where a_k is either 1 or −1, and $b_k \in \{-l_L, \ldots 1, 0, \ldots l_U\}$. The larger the numbers l_L, l_U, and L, the closer the SOPOT approximation will be to the original real number. In practice, the number of non-zero terms is usually kept to a small number while satisfying a given specification so that the multiplication can be implemented as limited numbers of shift and add (subtract) operations, giving rise to multiplier-less realization.

To reduce the number of adders for implementing $\alpha(z)$ and $\beta(z)$ as MB, we have to implement $\alpha(z)$ and $\beta(z)$ in their transposed form. In this case, instead of multiplying the delayed input samples with the filter coefficients as in the direct form, the input sample is now multiplied with all the filter coefficients. This can be efficiently implemented using a multiplier block. Let's consider a simple example with two filter coefficients: 3 and 21. The SOPOT representations of these two numbers are: $3 = 2^1 + 1$ and $21 = 2^4 + 2^2 + 1$. This requires 3 adders and 3 shifts. If implemented in a MB, the multiplication of the input with the coefficient 3 will also be generated by decomposing 3 as $2^1 + 1$, requiring one addition. The multiplication with 21, however, can be simplified by re-using the intermediate result generated by the first filter coefficient '3' as $21 = 3 \cdot 7 = 3 \cdot (2^4 - 1)$. Actually, the intermediate result, after multiplication by 3, is multiplied by 7, which requires one less

adder than generating 21 directly. In principle, it is possible to remove all the redundancy found in the constant multipliers leading to a realization with the *minimum number of adders*. This can drastically reduce the number of adders required for realizing such FBs when there are large numbers of filter coefficients to be implemented in the transposed form FIR structure [4].

III. DESIGN PROCEDURE AND EXAMPLES

We now introduce a new design method, called random search technique, to search for the SOPOT filter coefficients. The optimization procedure consists of two stages. First, a random search algorithm, to be discussed in the sequel, is used to search for the SOPOT coefficients of $\alpha(z)$ and $\beta(z)$ such that a given performance measure is minimized. Then, the minimum number of adders needed in the MB is determined. The generation of the MB from the SOPOT coefficients follows the algorithms proposed in [4]. Let $\boldsymbol{x}_I$ be the vector containing the real-valued coefficients of $\alpha(z)$ and $\beta(z)$ obtained by the method in [5]. The principle of the random search algorithm is to generate randomly candidate SOPOT coefficients in the neighborhood of $\boldsymbol{x}_I$ so as to search for the optimal discrete solution. More precisely, a new coefficient vector $\boldsymbol{x}_{NEW}$ is generated by adding to it a random vector to the original coefficient vector $\boldsymbol{x}_I$ as follows

$$\boldsymbol{x}_{NEW} = [\boldsymbol{x}_I + \alpha \cdot \boldsymbol{x}_R]_{SOPOT}, \tag{2}$$

where α is a scale factor which controls the size of the neighborhood to be searched, $\boldsymbol{x}_R$ is a vector with its elements being random numbers in the range $[-1,1]$, and $[\cdot]_{SOPOT}$ is the rounding operation which converts its argument to the nearest SOPOT coefficients with maximum number of terms in each coefficient being L and dynamic range l_U and l_L. The following objective function, which is the minimax error between the desired frequency response $H_d(e^{j\omega})$ and the frequency response $H(e^{j\omega}, \hat{\mathbf{x}})$ calculated using the candidate $\hat{\mathbf{x}}$ in the frequency band of interest $\omega \in S$, is minimized:

$$score = \max_{\omega \in S} \left(\left| H(e^{j\omega}, \hat{\boldsymbol{x}}) - H_d(e^{j\omega}) \right| \right). \tag{3}$$

The process is repeated with different vector $\hat{\mathbf{x}}$ so that the SOPOT space in the neighborhood of $\hat{\mathbf{x}}$ is sampled randomly. Since the sampled solutions are close to the real-valued optimal solution, their frequency responses will also be close to the ideal one, but with different hardware complexity. The set that yields the minimum score with a given number of terms is recorded. As this is a random search algorithm, the longer the searching time, the higher the chance of finding the optimal solution. There are several advantages of this algorithm. First of all, with the computational power of nowadays personal computer (PC) the time for obtaining high quality solutions is manageable, especially when an initial real-valued solution is available by some means. In fact, for the problem considered here, the overall design time is less than 5 minutes using a Pentium-400 PC with Matlab 5.3, including both the design of SOPOT coefficients and the MB. Secondly, it is applicable to problem with general objective function probably with very complicated inequality constraints. Moreover, a set of possible solutions representing different tradeoffs between computational complexity and performance will be generated during the search. Therefore, it helps one to achieve an appropriate tradeoff for a given application. It is also possible to combine the searching and the MB generation processes together for better performance but the computational time will be greatly increased.

Example 3.1

Here, we consider a low-delay FIR FB with N and M in fig. 5 chosen to be 3 and 8, respectively. Both $\alpha(z)$ and $\beta(z)$ are nonlinear-phase FIR filters. The cutoff-frequencies of the analysis filters are 0.4π and 0.6π, respectively. The filter coefficients are first calculated from the method in [5]. The SOPOT coefficient is then obtained using the random search algorithm described previously, and they are given in table 1. It can be seen from fig. 1 (their frequency responses) that the stopband attenuation of this FB is around 40dB. The searching time, including the design of the MB is less than 5 minutes in a Pentium-400 PC. The required number of adders in the MB for $\beta(z)$ is 10, 8 less than the direct implementation. For $\alpha(z)$, the number of adders required for the MB is 9, again 5 less than the direct implementation. The final implementation requires only 19 adders, saving 13 adders. In other words, a saving of 13/32 = 40.6 % of the original adders is achieved by using the MB. Fig. 2 shows the resultant MB for $\alpha(z)$. Another point worth mentioning is that both MBs are minimum-adder-graph [2], which means that they require the *least number of adders* to perform the required multiplication. Next, we consider their generalizations to 2D nonseparable FBs.

IV. 2D MULTIPLIER-LESS NONSEPARABLE PR FBs

Let $x(\boldsymbol{n})$ be a N-dimensional discrete-time signal with $\boldsymbol{n} = (n_0, \cdots, n_{N-1})^T$ and $n_i \in \aleph$, the set of integers. The output $y(\boldsymbol{n})$ of a decimator with an integer sub-sampling matrix $\boldsymbol{M}$ can be written as $y(\boldsymbol{n}) = x(\boldsymbol{Mn})$. The decimation factor is equal to $\boldsymbol{D} = |\det(\boldsymbol{M})|$. Different choices of $\boldsymbol{M}$ give rise to different spectral support of $x(\boldsymbol{n})$ in order to achieve aliasing-free decimation. The points in $x(\boldsymbol{n})$ that are retained in $y(\boldsymbol{n}) = x(\boldsymbol{Mn})$ lie on the lattice $\{LAT(\boldsymbol{M}) : \boldsymbol{t} = \boldsymbol{Mn}, \boldsymbol{n} \in \aleph^N\}$. Fig. 4c shows the lattice generated by the 2D sampling matrix $\boldsymbol{M}_Q = [\boldsymbol{M}_{Q\_0} \quad \boldsymbol{M}_{Q\_1}]$ associated with the quincunx spectral support in fig.4a where $\boldsymbol{M}_{Q\_0} = [1 \quad 1]^T$ and $\boldsymbol{M}_{Q\_1} = [1 \quad -1]^T$. It can also be seen that those points on $LAT(\boldsymbol{M})$ are in fact generated by the linear combinations of $\boldsymbol{M}_{Q\_0}$ and $\boldsymbol{M}_{Q\_1}$. Fig. 6 shows the general structure of a two-channel critically decimated MD FB with sub-sampling matrix $\boldsymbol{M}$ and $|\det(\boldsymbol{M})| = 2$. The analysis and synthesis filters have been written respectively in their type-I and type-II polyphase representations with $\boldsymbol{E}(z^{\boldsymbol{M}})$ and $\boldsymbol{R}(z^{\boldsymbol{M}})$ their polyphase matrices. $\boldsymbol{k}_0$ and $\boldsymbol{k}_1$ are the set of integer vectors, $\aleph(\boldsymbol{M})$, which lie inside the fundamental parallelepiped of $\boldsymbol{M}$, $FPD(\boldsymbol{M})$, where $FPD(\boldsymbol{M})$ is the region spanned by $\boldsymbol{M} \cdot \boldsymbol{x}$, with $x_i \in [0,1), i = 0,\ldots,N-1$. The gray parallelogram area in Fig. 4c spanned by the two vectors $(\boldsymbol{M}_{Q\_0}, \boldsymbol{M}_{Q\_1})$ is the $FPD(\boldsymbol{M})$ associated with $\boldsymbol{M}_Q$. The corresponding values of $\boldsymbol{k}_0$ and $\boldsymbol{k}_1$ are seen to be $\boldsymbol{k}_0 = [0 \quad 0]^T$ and $\boldsymbol{k}_1 = [1 \quad 0]^T$. If the product $\boldsymbol{R}(z^{\boldsymbol{M}})\boldsymbol{E}(z^{\boldsymbol{M}})$ is equal to a constant multiplies of signal delay, then the system is PR. A simple method for achieving this condition is by transformation of 1D PR FB [2], like the one we have designed in sections II and III. More precisely, in [2], both $\alpha(z^2)$ and $\beta(z^2)$ are equal and they are transformed to $\beta(z^{M_0})\beta(z^{M_1})$. The 1-D delay z^2 is then replaced with $z^{M_0}z^{M_1}$. Careful examination shows that a similar transformation can be carried out if $\alpha(z^2)$ and $\beta(z^2)$ are *unequal*. In fact, they can be transformed respectively to

$\alpha(z^{M_0})\alpha(z^{M_1})$ and $\beta(z^{M_0})\beta(z^{M_1})$. Then, the 2D analysis filters are $H_0(z_0,z_1)=\frac{1}{2}\left((z^{M_0}z^{M_1})^{-N}+z^{-k_1}\beta(z^{M_0})\beta(z^{M_1})\right)$ and $H_1(z_0,z_1)=-\alpha(z^{M_0})\alpha(z^{M_1})H_0(z_0,z_1)+z^{-k_1}(z^{M_0}z^{M_1})^{-M}$. The resultant FB is shown in fig. 6. For the quincunx spectral support we have $z^{M_{Q\_0}}=z_0z_1$, $z^{M_{Q\_1}}=z_0z_1^{-1}$, $z^{M_Q}=z_0^2$, and

$$H_0(z_0,z_1)=\frac{1}{2}\left(z_0^{-2N}+z_0^{-1}\beta(z_0z_1)\beta(z_0z_1^{-1})\right),$$

$$\text{and } H_1(z_0,z_1)=-\alpha(z_0z_1)\alpha(z_0z_1^{-1})H_0(z_0,z_1)+z_0^{-2M-1}. \quad (4)$$

It should be noted that this transformation is also valid if $\alpha(z)$ and $\beta(z)$ are linear-phase/nonlinear-phase FIR and IIR functions. To design a PR FB with a hourglass spectral support, we can multiply $x(n)$ and $\hat{x}(n)$ in the quincunx PR FB by $(-1)^{n_1}$ [1]. The design of a PR nonseparable FB with a parallelogram support as shown in fig. 4b is slightly more complicated because we need to determine the form of its sampling matrix, M_P, the integer vectors k_0, k_1, and hence the parameters of the transformation. First of all, it is noted that the spectral support Ω of the analysis lowpass filter should be equal to the aliasing-free spectral support of $x(n)$ if decimated by M_P. This is given by [10], $\{\Omega:\omega=\pi M^{-T}x, x\in[-1,1)^2\}$. For notational convenience, let $\pi M^{-T}=[\omega_0,\omega_1]$. Consider the quincunx sampling as an example, the spectral support is a parallelogram defined by the two vectors, $\omega_0=[\pi/2 \quad \pi/2]^T$ and $\omega_1=[-\pi/2 \quad \pi/2]^T$ (fig.4a). In general, if $[\omega_0,\omega_1]$ can be determined from the desired spectral support, then M can be computed from $\mathbf{M}=[\omega_0 \quad \omega_1]^{-T}/\pi$. Using this formula, one can easily verified that the sampling matrix of the quincunx spectral support is given by $M_Q=\begin{bmatrix}1 & 1\\ 1 & -1\end{bmatrix}$. The calculation of parallelogram support is similar. In fact, we have $\omega_0=[\pi/2 \quad 0]^T$ and $\omega_1=[-\pi/2 \quad \pi]^T$ and $M_P=[M_{P\_0} \quad M_{P\_1}]$, where $M_{P\_0}=[2 \quad -1]^T$ and $M_{P\_1}=[0 \quad 1]^T$. k_0 and k_1 are determined to be $k_0=[0 \quad 0]^T$ and $k_1=[1 \quad 0]^T$. The analysis filters are then given by

$$H_0(z_0,z_1)=\frac{1}{2}\left(z_0^{-2N}+z_0^{-1}\beta(z_0z_1)\beta(z_0z_1^{-1})\right),$$

$$\text{and } H_1(z_0,z_1)=-\alpha(z_0z_1)\alpha(z_0z_1^{-1})H_0(z_0,z_1)+z_0^{-2M-1}. \quad (5)$$

We now present some design examples.

Example 4.1

The 1-D low-delay multiplier-less PR FB obtained in Example 3.1 is transformed using equations (4) and (5) derived in the previous section to obtain the corresponding 2D multiplier-less FBs with Quincunx and parallelogram spectral support as shown in Fig. 4. The FB with hourglass shape spectral support is obtained by shifting the frequency spectrum of the quincunx FB via the modulation $e^{j\pi n_1}$, where n_1 is the integer index in the vertical direction. (Interested readers are refer to [1] for more details). The contour plots of their frequency responses are shown in fig. 7. The design of PR FBs with parallelogram spectral support at orientations of 150, 240 and 330 degrees are similar (the one shown in fig. 7c has a orientation of 60 degrees). By properly cascading these sets of basic PR FBs in a tree structure, as suggested in [1], it is possible to realize new multiplier-less PR directional FBs with very low implementation and design complexities. Due to page limitation, interested readers are referred to [1] for more details of the actual arrangement and their applications in directional image decomposition and motion analysis.

V. CONCLUSION

A new design and implementation method for a class of multiplier-less 2-channel 1D and 2D non-separable perfect reconstruction (PR) filter banks (FB) is presented. It is based on the structure proposed by Phoong et al and the use of multiplier block (MB). The latter technique allows one to further reduce the number of adders in implementing these multiplier-less FB by almost 50%, compared to the conventional method using sum of powers of two coefficients (SOPOT) alone. Furthermore, by generalizing the 1D to 2D transformation of Phoong *et al.*, new 2D PR FB with Quincunx, hourglass, and parallelogram spectral support are obtained. These nonseparable FBs can be cascaded to realize new multiplier-less PR directional FB for image processing and motion analysis. Design examples are given to demonstrate the usefulness of the proposed method.

REFERENCES

[1] R. H. Bamberger, and M. J. T Smith, "A filter bank for the directional decomposition of images: theory and design," *IEEE Trans. Signal Processing*, vol. 40, pp. 882-893, Apr. 1992.

[2] S. M. Phoong, C. W. Kim, P.P. Vaidyanathan, and R. Ansari, "A new class of two-channel biothogonal filter banks and wavelet bases," *IEEE Trans. Signal Processing*, vol. 43, pp. 649-664, Mar. 1995.

[3] Y.C. Lim and S. R. Parker, "FIR filter design over a discrete power-of-two coefficient space," *IEEE Trans. Acoust. Speech, Signal Processing*, vol. ASSP-31, pp. 583-591, June 1983.

[4] A. G. Dempster and M. D. Macleod, "Use of minimum-adder multiplier blocks in FIR digital filters," *IEEE Trans. CAS-II*, vol. 42, pp. 569-577, Sep. 1995.

[5] J. S. Mao, S. C. Chan and K. L. Ho, "Design and multiplier-less implementation of a class of two-channel PR FIR filter banks with low system delay," *IEEE Trans. Signal Processing*, vol. 48, pp. 3379-3394, Dec. 2000.

[6] W. Liu, S. C. Chan, and K. L. Ho, "Multiplier-less low-delay FIR and IIR wavelet filter banks with SOPOT coefficients," in *Proc. IEEE Int. Conf. Acoust. Speech, Signal Process. (ICASSP)*, Istanbul, Turkey, May. 2000.

[7] S. Sriranganathan, D. R. Bull, and D. W. Redmill, "The design of low complexity two-channel lattice-structure perfect-reconstruction filter banks using genetic algorithms," in *Proc. IEEE Int. Symp. Circuits Syst. (ISCAS)*, Jun. 1997.

[8] I. Daubechies and W. Sweldens, "Factoring wavelet transform into lifting steps," *J. Fourier Anal. Appl.*, vol. 4, pp. 247-269, 1998.

[9] D. Pinchon, and P. Siohan, "Analysis, design, and implementation of two-channel linear-phase filter banks: a new approach," *IEEE Trans. on Signal Processing*, vol. 46, pp. 1814 –1826, 1998.

[10] P. P. Vaidyanathan, *Multirate Systems and Filter Banks*. Englewood Cliffs, NJ: Prentice Hall, 1993.

	$H_0(z)$ (–39.084dB), avg. no. of term = 2.38	$H_1(z)$ (–39.48dB), avg. no. of term = 2.13
n	$\beta(z)$	$\alpha(z)$
0	$2^{-5}+2^{-7}$	-2^{-7}
1	$-2^{-3}+2^{-6}-2^{-8}$	$2^{-5}-2^{-7}$
2	$2^{-1}+2^{-5}+2^{-8}$	$-2^{-4}+2^{-6}-2^{-8}$
3	$2^{0}-2^{-2}-2^{-6}$	$2^{-4}+2^{-6}+2^{-8}$
4	$-2^{-2}-2^{-4}+2^{-7}$	$-2^{-2}+2^{-4}+2^{-7}$
5	$2^{-2}-2^{-3}-2^{-7}$	$2^{-1}+2^{-3}-2^{-6}$
6	$-2^{-3}-2^{-5}$	$2^{-1}+2^{-3}+2^{-5}$
7	$2^{-3}-2^{-7}$	$-2^{-2}+2^{-5}$
8	$-2^{-3}+2^{-5}+2^{-8}$	$2^{-3}-2^{-9}$
9	2^{-4}	$-2^{-4}-2^{-6}$
10	$-2^{-5}-2^{-6}+2^{-8}$	$2^{-4}-2^{-6}+2^{-9}$
11	$2^{-5}-2^{-7}$	$-2^{-5}+2^{-8}$
12	-2^{-6}	2^{-6}
13		-2^{-7}
14		2^{-8}

Table 1. Filter coefficients for Example 3.1.

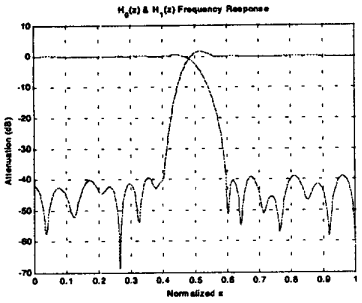

Figure 1. Frequency response of the SOPOT FB in Example 3.1.

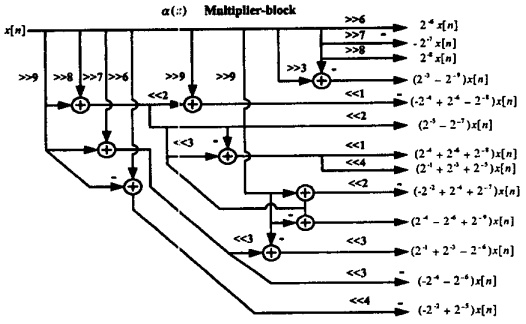

Figure 2. Multiplier-block for $\alpha(z)$ in Example 3.1.
("$>>x$" means shift x no. of bits towards the LSB while "$<<x$" means shift x no. of bits towards the MSB)

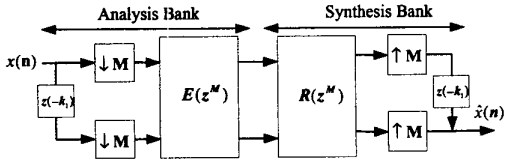

Figure 3. The multidimensional maximally decimated 2-channel FB.

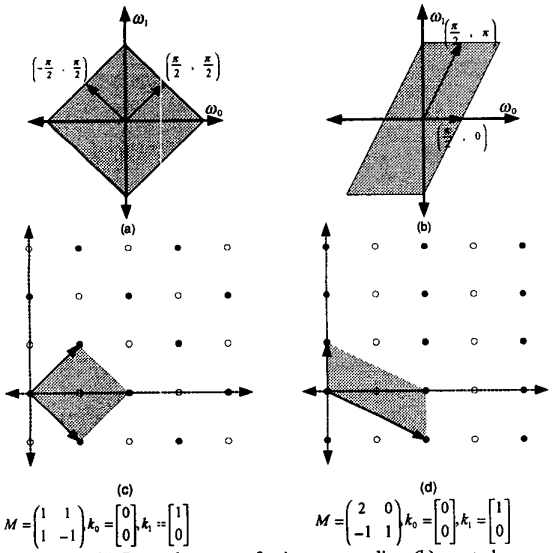

$$M=\begin{pmatrix}1 & 1\\ 1 & -1\end{pmatrix}, k_0=\begin{bmatrix}0\\0\end{bmatrix}, k_1=\begin{bmatrix}1\\0\end{bmatrix} \qquad M=\begin{pmatrix}2 & 0\\ -1 & 1\end{pmatrix}, k_0=\begin{bmatrix}0\\0\end{bmatrix}, k_1=\begin{bmatrix}1\\0\end{bmatrix}$$

Figure 4. (a) Spectral support of quincunx sampling, (b) spectral support for the parallelogram filter, (c) sampling matrix and its associated lattice for quincunx sampling, (d) sampling matrix and its associated lattice for the parallelogram filter.

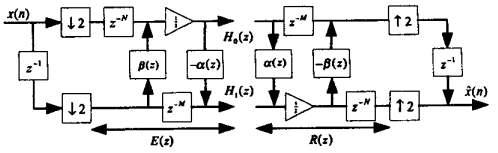

Figure 5. The PR FB in [2].

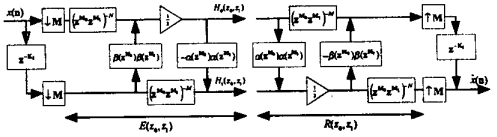

Figure 6. 2D PR 2-channel FB after transformation of variables.

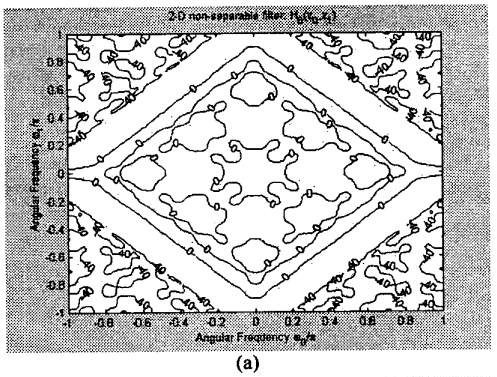

(a)

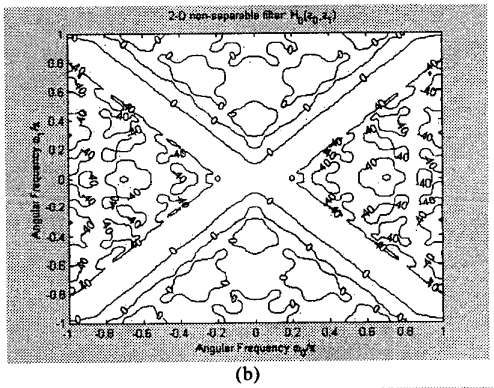

(b)

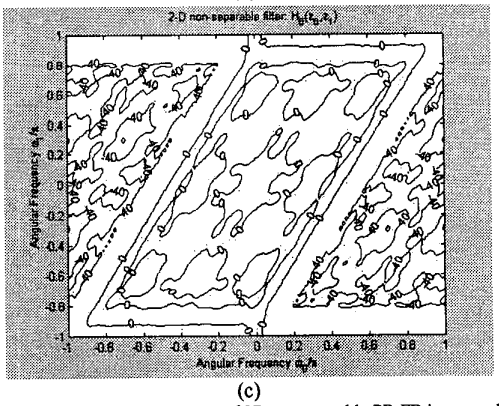

(c)

Figure 7. Frequency responses of 2D nonseparable PR FB in example 4.1. : (a) Quincunx, (b) Hourglass, and (c) Parallelogram.